REPORT DOCUMENTATION PAGE

Form Approved OMB NO. 0704-0188

1. REPORT DATE (DD-MM-YYYY)	2. REPORT TYPE	3. DATES COVERED (From - To)
	New Reprint	-

4. TITLE AND SUBTITLE
Poly(2,6-dimethyl-1,4-phenylene oxide) Blended with Poly (vinylbenzyl chloride)-

5a. CONTRACT NUMBER
W911NF-10-1-0520

5b. GRANT NUMBER

5c. PROGRAM ELEMENT NUMBER
611103

6. AUTHORS
Yifan Li, Aaron C. Jackson, Frederick L. Beyer, Daniel M. Knauss

5d. PROJECT NUMBER

5e. TASK NUMBER

5f. WORK UNIT NUMBER

7. PERFORMING ORGANIZATION NAMES AND ADDRESSES
Colorado School of Mines
1500 Illinois St

Golden, CO 80401 -1911

8. PERFORMING ORGANIZATION REPORT NUMBER

9. SPONSORING/MONITORING AGENCY NAME(S) AND ADDRESS (ES)
U.S. Army Research Office
P.O. Box 12211
Research Triangle Park, NC 27709-2211

10. SPONSOR/MONITOR'S ACRONYM(S)
ARO

11. SPONSOR/MONITOR'S REPORT NUMBER(S)
58161-CH-MUR.55

12. DISTRIBUTION AVAILIBILITY STATEMENT
Approved for public release; distribution is unlimited.

13. SUPPLEMENTARY NOTES
The views, opinions and/or findings contained in this report are those of the author(s) and should not contrued as an official Department of the Army position, policy or decision, unless so designated by other documentation.

14. ABSTRACT
A block copolymer of poly(vinylbenzyl chloride)-b-polystyrene (PVBC-b-PS) was synthesized through nitroxide-mediated polymerization, then blended with poly(2,6-dimethyl-1,4-phenylene oxide) (PPO) at different compositions, and solution cast to prepare a series of blend films. Differential scanning calorimetry analysis of the PVBC-b-PS and PVBC-b-PS blended with the PPO showed a single glass transition temperature for each of the compositions examined, suggesting that all components in the blend membranes are compatible. The benzyl chloride groups in the blend films were converted to quaternary ammonium groups by reaction with

15. SUBJECT TERMS
Anion Exchange Membrane, Polymer synthesis, SAXS, Polymer tensile testing

16. SECURITY CLASSIFICATION OF:			17. LIMITATION OF ABSTRACT	15. NUMBER OF PAGES	19a. NAME OF RESPONSIBLE PERSON
a. REPORT	b. ABSTRACT	c. THIS PAGE			Andrew Herring
UU	UU	UU	UU		19b. TELEPHONE NUMBER 303-384-2082

Report Title

Poly(2,6-dimethyl-1,4-phenylene oxide) Blended with Poly(vinylbenzyl chloride)-

ABSTRACT

A block copolymer of poly(vinylbenzyl chloride)-b-polystyrene (PVBC-b-PS) was synthesized through nitroxide-mediated polymerization, then blended with poly(2,6-dimethyl-1,4-phenylene oxide) (PPO) at different compositions, and solution cast to prepare a series of blend films. Differential scanning calorimetry analysis of the PVBC-b-PS and PVBC-b-PS blended with the PPO showed a single glass transition temperature for each of the compositions examined, suggesting that all components in the blend membranes are compatible. The benzyl chloride groups in the blend films were converted to quaternary ammonium groups by reaction with trimethylamine, and the functionalization reached high conversion as characterized by ion exchange capacity (IEC) measurements. The PPO blend anion exchange membranes (AEMs) show improved mechanical properties compared to the styrenic copolymer, particularly in a hydrated condition. The membranes were subjected to thermal and THF/water annealing procedures to study the effect on membrane properties. Small-angle X-ray scattering (SAXS) experiments indicated the formation of a phase separated morphology in the membrane after annealing with solvent vapor in the presence of water. The ionic conductivities of the blended membranes show an expected increase with increasing IEC and corresponding water uptake. Ionic conductivity and water uptake were found to increase significantly after either annealing in the presence of water and THF or high-temperature annealing in the presence of water. The highest hydroxide conductivity reached 43 mS/cm measured at 60 °C in water.

REPORT DOCUMENTATION PAGE (SF298)
(Continuation Sheet)

Continuation for Block 13

ARO Report Number 58161.55-CH-MUR
Poly(2,6-dimethyl-1,4-phenylene oxide) Blendec...

Block 13: Supplementary Note

Approved for public release; distribution is unlimited.

Macromolecules

Article

pubs.acs.org/Macromolecules

Poly(2,6-dimethyl-1,4-phenylene oxide) Blended with Poly(vinylbenzyl chloride)-*b*-polystyrene for the Formation of Anion Exchange Membranes

Yifan Li,[†] Aaron C. Jackson,[‡] Frederick L. Beyer,[‡] and Daniel M. Knauss*[,†]

[†]Department of Chemistry and Geochemistry, Colorado School of Mines, Golden, Colorado 80401, United States

[‡]Weapon & Materials Research Directorate, US Army Research Laboratory, Aberdeen Proving Ground, Maryland 21005, United States

ABSTRACT: A block copolymer of poly(vinylbenzyl chloride)-*b*-polystyrene (PVBC-*b*-PS) was synthesized through nitroxide-mediated polymerization, then blended with poly(2,6-dimethyl-1,4-phenylene oxide) (PPO) at different compositions, and solution cast to prepare a series of blend films. Differential scanning calorimetry analysis of the PVBC-*b*-PS and PVBC-*b*-PS blended with the PPO showed a single glass transition temperature for each of the compositions examined, suggesting that all components in the blend membranes are compatible. The benzyl chloride groups in the blend films were converted to quaternary ammonium groups by reaction with trimethylamine, and the functionalization reached high conversion as characterized by ion exchange capacity (IEC) measurements. The PPO blend anion exchange membranes (AEMs) show improved mechanical properties compared to the styrenic copolymer, particularly in a hydrated condition. The membranes were subjected to thermal and THF/water annealing procedures to study the effect on membrane properties. Small-angle X-ray scattering (SAXS) experiments indicated the formation of a phase-separated morphology in the membrane after annealing with solvent vapor in the presence of water. The ionic conductivities of the blended membranes show an expected increase with increasing IEC and corresponding water uptake. Ionic conductivity and water uptake were found to increase significantly after either annealing in the presence of water and THF or high-temperature annealing in the presence of water. The highest hydroxide conductivity reached 43 mS/cm measured at 60 °C in water.

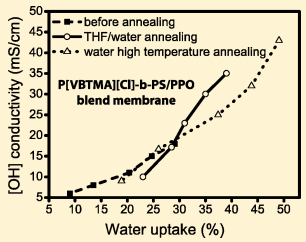

INTRODUCTION

Alkaline fuel cells (AFCs) using anion exchange membranes (AEMs) as electrolyte have recently received considerable attention.[1,2] AFCs offer some advantages over proton exchange membrane (PEM) fuel cells, including the potential to use non-noble metal (e.g., nickel, silver)[3] catalysts on the cathode, which can dramatically lower the fuel cell cost. The main drawback of traditional AFCs is the use of liquid electrolyte (e.g., aqueous KOH), which can result in the formation of carbonate precipitates by reaction with carbon dioxide.[4−6] AEMs with bound cationic functional groups eliminate the precipitates formed in traditional AFCs.[2,7]

In order to have useful AEMs for AFC applications, a robust membrane with high ionic conductivity and good mechanical properties that can be operated in a high pH environment is required. Therefore, it is important to investigate a variety of cationic functional groups and polymer compositions. The most widely studied AEMs contain quaternary ammonium functional groups,[8] which are relatively simple to effect functionalization and have demonstrated moderate alkaline stability.[9] The polymer backbone chain structure is an additional important component of AEMs. Efforts have been directed to develop various polymer backbones for AEMs containing quaternary ammonium cations, including poly(arylene ether)s,[10−13] poly(phenylene),[14] polyethylene,[15,16] and polystyrene derivatives.[17−20] There is a particular interest in styrenic block copolymer structures because they can be readily synthesized and functionalized as well as the possibility to develop well-defined morphologies upon film formation.

Styrenic block copolymers are attractive materials for conversion into AEMs; however, their anticipated brittleness and other poor mechanical properties limit their potential. One method that may lead to improved mechanical properties of styrenic block copolymers is to blend with poly(2,6-dimethyl-1,4-phenylene oxide) (PPO). PPO is an engineering plastic with high strength, chemical resistance,[21] and a high glass transition temperature ($T_g \approx 220$ °C).[22] PPO has also been widely used as a backbone polymer to prepare anion exchange membranes for fuel cell application by utilizing the pendent methyl groups for functionalization.[23−27] Furthermore, PPO is well-known to form miscible blends with polystyrene and some polystyrene copolymers.[28−34] Recently, PPO has been blended in polystyrene-based ionic polymers to prepare PEMs where the blended membrane shows improved thermal stability and limited water uptake.[35,36] However, research has not been done on blending styrenic block copolymers with PPO as a means of improving properties of the materials for AEMs.

Received: May 13, 2014
Revised: August 14, 2014

   dx.doi.org/10.1021/ma500993s | *Macromolecules* XXXX, XXX, XXX−XXX

In the current study, we demonstrate a methodology to prepare PPO blended polystyrene-based AEMs. The formation of the membrane involves the synthesis of poly(vinylbenzyl chloride)-*b*-polystyrene (PVBC-*b*-PS) by nitroxide-mediated polymerization, followed by solvent casting of PVBC-*b*-PS/PPO blends from chloroform, and subsequently reacting the PVBC-*b*-PS/PPO blend films with trimethylamine to convert the benzyl chloride pendent groups into quaternary ammonium cationic groups. A series of PPO blended membranes are prepared, and the cationic functionality or ionic exchange capacity is tuned by varying the PPO content of the membrane. The research investigates in detail the preparation of the polymer blend membranes and the effect of PPO on the membrane properties including water uptake, ionic conductivity, and mechanical properties. Additionally, the blend membranes are annealed by thermal and solvent vapor methods to study the effect on water uptake, ionic conductivity, and morphology.

EXPERIMENTAL SECTION

Materials. Styrene (99%) and 4-vinylbenzyl chloride (VBC) (90%) were obtained from Aldrich, dried over calcium hydride, and distilled under reduced pressure right before use. 2,2,6,6-Tetramethylpiperidine-1-oxyl (TEMPO) (Aldrich, 98%) was sublimed twice before use. Anhydrous trimethylamine gas (99%) was used as received. Benzoyl peroxide (BPO) was purified by recrystallization from chloroform/methanol. PPO homopolymer was purchased from Aldrich (M_n = 20 000 g/mol) and used as received.

Synthesis of PVBC-*b*-PS by Nitroxide-Mediated Polymerization (NMP). All glassware was dried at ∼150 °C overnight before the polymerization. The purified VBC (20.0 mL), BPO (56 mg, 0.2 mmol), and TEMPO (62 mg 0.4 mmol) were added into a 50 mL round-bottom flask containing a magnetic stir bar and capped with a rubber septum. After dissolution, the round-bottom flask was purged with Ar for 30 min. The mixture was heated to 125 °C for 3 h to allow for polymerization. The TEMPO-terminated PVBC (PVBC-TEMPO) was purified by several precipitations in methanol and further dried in a vacuum oven before use. PVBC-TEMPO was then used as a macroinitiator to copolymerize styrene in a bulk polymerization. PVBC-TEMPO (250 mg) was weighed into a 50 mL round-bottom flask, and an excess of styrene (10 mL) was injected into the flask. After PVBC-TEMPO was dissolved in styrene, the round-bottom flask was purged with Ar for 30 min. The bulk polymerization was carried out at 125 °C for 30 min. The copolymer was isolated by precipitation in methanol and was purified by reprecipitating after redissolving in chloroform. The copolymer was then dried under vacuum at room temperature.

PPO Blended AEM Preparation. PPO and PVBC-*b*-PS materials were dried in a vacuum oven before blending and then dissolved together in chloroform under sonication with a range of different mass ratios (PVBC-*b*-PS:PPO = 40:60, 50:50, 60:40, 70:30, and 80:20). All blend concentrations were prepared at 5 g/100 mL. Polymer blend solutions were drop cast by a pipet onto glass slides, and the solvent was allowed to evaporate slowly at room temperature. The glass slide was immersed in deionized water to remove the polymer film. All films (PVBC-*b*-PS/PPO) obtained were transparent. PVBC-*b*-PS/PPO films were then rinsed with methanol and soaked in round-bottom flasks filled with methanol. A 500% excess of anhydrous trimethylamine gas was introduced to the round-bottom flask and allowed to react over 48 h at room temperature to convert PVBC-*b*-PS/PPO films into poly(vinylbenzyltrimethylammonium chloride)-*b*-polystyrene/PPO (P[VBTMA][Cl]-*b*-PS/PPO). The PPO blend membranes containing quaternary ammonium cations were soaked repeatedly with methanol and then deionized water. All quaternized membranes were dried in a vacuum oven at 60 °C overnight.

Membrane Annealing. Annealing was attempted on membrane samples in the ammonium chloride form. Each membrane sample was cut into five pieces. One piece was retained for characterization without annealing, and the four remaining pieces were subjected to one of four annealing methods: (1) membranes were suspended in boiling deionized water for 12 h; (2) membranes were annealed at 125−140 °C under dry conditions for 12 h; (3) membranes were annealed at 125−140 °C with deionized water for 12 h in a sealed pressure vessel; and (4) membranes were annealed in a sealed pressure vessel at 70 °C over a 50/50 THF/water solution for 12 h. Quaternized blend membranes were dried in a vacuum oven after annealing.

Ion Exchange to Hydroxide. The P[VBTMA][Cl]-*b*-PS/PPO membranes were soaked in 1 M KOH solution for 48 h at room temperature to exchange chloride to hydroxide and were subsequently rinsed repeatedly with degassed deionized water to remove residual salts.

Characterization. Molecular weights of PVBC-TEMPO and PVBC-*b*-PS were determined by gel permeation chromatography (GPC) using a Waters HPLC pump equipped with a Wyatt Technology Optilab RI detector and a Wyatt Technology miniDAWN multiangle laser light scattering (MALLS) detector. Elutions were carried out with two Polymer Laboratories Mixed-D columns at room temperature with THF at a flow rate of 1.0 mL/min, and the molecular weights were measured by calibration of a series of polystyrene standards and also using software (Astra) supplied by Wyatt Technology. ^{1}H NMR spectra of PVBC-*b*-PS in $CDCl_3$ were obtained using a JEOL 500 MHz spectrometer. IR measurements were performed on a Thermo FT-IR spectrometer in a spectral range of 500−4000 cm^{-1}. Glass transition temperatures (T_g) of blend membranes were measured by differential scanning calorimetry (DSC) on a TA Instruments DSC-20 running TA software with a heating rate of 10 °C/min under a nitrogen atmosphere. Thermal stability was determined by thermogravimetric analysis (TGA) on a Seiko TGA/DTA320 at a heating rate of 10 °C/min under a nitrogen atmosphere.

Theoretical ionic exchange capacities (IECs) were calculated based on 100% conversion of benzyl chloride to quaternary ammonium. IECs of blend membranes in their hydroxide form were experimentally determined by using an established literature titration method.[37] About 0.02 g of vacuum-dried blend membranes in the hydroxide form was immersed in 10.00 mL of 0.009 87 M standardized HCl solution for 48 h; the actual IEC was calculated by titration of unreacted HCl with 0.010 53 M standardized NaOH solution. The titrations were repeated three times for each blend membrane. The IEC (mmol/g) was obtained by

$$\text{IEC (mmol/g)} = \frac{M_{0\text{ h,HCl}} - M_{48\text{ h,HCl}}}{m_{\text{dry membrane}}}$$

where $M_{0\text{ h,HCl}}$ is millimoles (mmol) of HCl determined before the blend membrane neutralization, $M_{48\text{ h,HCl}}$ is mmol determined after neutralization of membranes (after 48 h), and $m_{\text{dry membrane}}$ is the dry mass (g) of membrane in the hydroxide form.

Water uptake of AEMs was determined by established methods.[38] Membranes were presoaked in deionized water, and after 24 h of soaking, the fully hydrated membranes were removed from the water; any residual bulk water on the membrane surface was blotted dry with Kimwipes, and the sample was weighed immediately. The membranes were immersed again into deionized water for another 15 min to let them rehydrate. This method was repeated five times to obtain the average mass of hydrated membranes (m_{hydrated}). The membranes were subsequently vacuum-dried at 60 °C for 24 h to obtain a dry mass (m_{dry}). The water uptake (WU) was determined by

$$\text{WU (\%)} = \frac{m_{\text{hydrated}} - m_{\text{dry}}}{m_{\text{dry}}} \times 100\%$$

Synchrotron small-angle X-ray scattering (SAXS) experiments were performed at the Advanced Photon Source at Argonne National Laboratory. A beam energy of 12 keV with X-ray wavelength, λ, of 1.03 Å was employed to measure samples in transmission mode. The transmission intensity was normalized to exposure time and flux of the direct beam through the sample. The films were held in place using

dx.doi.org/10.1021/ma500993s | Macromolecules XXXX, XXX, XXX−XXX

Scheme 1. Strategy of PPO Blended AEM Preparation

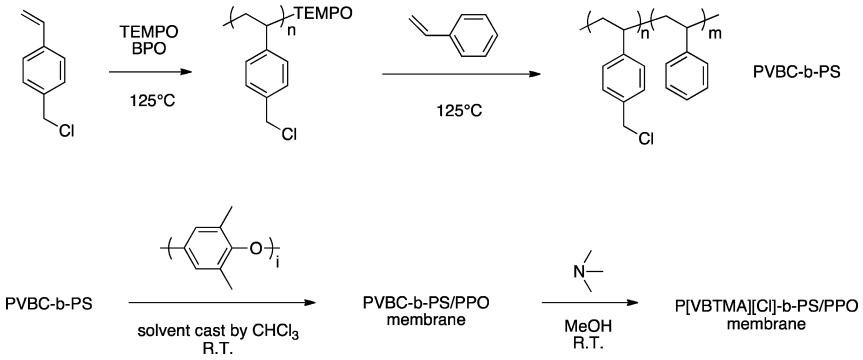

Kapton tape to the sample holder and placed in a custom-built four-sample oven that controlled the humidity and temperature of the samples during scattering experiments.[39,40] The humidity of the sample environment was controlled using a combination of wet and dry nitrogen with a humidity probe positioned in the sample oven to provide real time humidity readout. Based on the humidity measurement, gas flows were adjusted to achieve the desired temperature and humidity condition. Igor Pro was used to analyze the data. The 2D scattering patterns were azimuthally integrated to obtain intensity as a function of scattering vector magnitude, q, where $q = 4\pi \sin(\theta)/\lambda$ and 2θ is the scattering angle.

High-angle annular dark field scanning transmission electron microscopy (HAADF STEM) was performed at the US Army Research Laboratory. The blend membranes in chloride form were ion exchanged in 1 M potassium bromide solution for 48 h before sample preparation. Preparation of samples for transmission electron microscopy (TEM) was by cryo-ultramicrotomy. A Leica UCT microtome and a Microstar Tech diamond knife were used to collect sections approximately 70 nm thick. Imaging was performed using a JEOL USA, Inc., JEM-2100F field emission TEM operated at an accelerating voltage of 200 kV. Dark field images were collected using a Gatan, Inc., model 806 HAADF scintillation detector. HAADF STEM data were collected using a 40 μm condenser aperture, a probe size of 0.2 nm, and a camera length of 2 cm to maximize Z contrast.

The in-plane ionic conductivities of blend membranes were measured by four probe electrochemical impedance spectroscopy[41] using a BioLogic VMP3 potentiostat over a frequency of 0.1−10^6 Hz. The conductivity can be calculated from the membrane resistance

$$\sigma = \frac{l}{RA}$$

where R is the membrane resistance, l is the distance between the electrodes, and A is the cross-sectional area of the sample. The hydroxide and chloride conductivities were measured in water at room temperature and at 60 °C.

Tensile properties of blended membranes were measured under dry and hydrated conditions on an Instru-Met frame tensile tester using a 1000 lb load cell (with a resolution less than 0.1 lb) and a cross-head speed of 5 mm/min at room temperature. The dry samples were prepared by drying membranes in a vacuum oven at 60 °C for 24 h, and the hydrated samples were prepared by soaking membranes in deionized water at room temperature for 24 h. Blend membranes were cut into strips of approximately 60 mm × 8 mm, and membrane thicknesses were measured in a range of 50−80 μm. Stress was calculated from the cross-sectional area of the film, and the strain was obtained by the percentage increase of film gauge length. The Young's modulus was determined by the initial slope of the stress vs strain curve at very low strains (0.2−0.3%). Five replicates were performed on each sample to obtain the average values of stress, strain, and Young's modulus.

RESULTS AND DISCUSSION

Recently, block copolymers that form well-defined morphologies have attracted considerable attention in polymer electrolyte design,[41−43] and styrenic block copolymers have aroused interest for study as AEMs.[20,44,45] PS is believed to be quite stable under alkaline fuel cell conditions;[46] however, the poor flexibility of PS somewhat limits its use as a membrane material for fuel cell applications. PPO is a commercially available polymer, and the miscibility of PPO/PS blends has been well recognized for decades.[47] PPO is an engineering polymer with good mechanical properties, and a significant amount of research on PPO blends has been done to improve the mechanical properties of polystyrene and styrenic copolymers for different applications.[22,32,34,48−52] Here, a PPO blended AEM preparation method is designed where a PVBC-*b*-PS block copolymer is first synthesized and subsequently blended with PPO and then solvent cast to prepare blend films. The conversion of benzyl chloride groups into quaternary ammonium groups is accomplished through the reaction with trimethylamine, and the preparation steps are depicted in Scheme 1.

Numerous methods can be used to synthesize polystyrene-based block copolymers with controlled composition and relative segment length. Nitroxide-mediated polymerization (NMP) was selected to synthesize the diblock, since this technique has been demonstrated to effect the polymerization of VBC and offers the control over the relative composition.[53] The polymerization of VBC was carried out using BPO as radical initiator in the presence of TEMPO,[54,55] and then the resulting PVBC-TEMPO was used as macroinitiator to polymerize a styrene block. The PVBC with a TEMPO functional chain end (PVBC-TEMPO) was analyzed by GPC using THF as elution solvent to determine a M_n = 30 500 g/mol and M_w/M_n = 1.90. Several precipitations were conducted on PVBC-TEMPO in order to remove any remaining VBC monomer. The nitroxide-mediated copolymerization of styrene was initiated by the purified PVBC-TEMPO macroinitiator at 125 °C in bulk. The conversion of styrene reached ∼5% after 30 min of reaction. The results of GPC analysis of PVBC-TEMPO and PVBC-*b*-PS diblock copolymer are depicted in Figure 1.

The molecular weight of PVBC-*b*-PS was determined by GPC to find M_n = 85 700 g/mol and M_w/M_n = 1.86. The GPC chromatogram of PVBC-TEMPO shows a small amount of tailing to low molecular weights, resulting in the broad peak feature. The broad molecular weight distribution may be

dx.doi.org/10.1021/ma500993s | *Macromolecules* XXXX, XXX, XXX−XXX

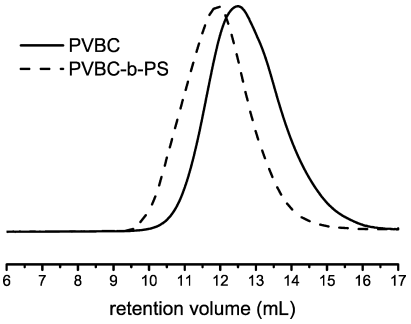

Figure 1. GPC curves (THF elution solvent) of TEMPO-functionalized PB and PB-*b*-PS diblock copolymer.

attributed to the high reactivity of VBC monomer and uncontrolled initiation by using TEMPO as an additive rather than preforming a nitroxide initiator.[56,57] After the block copolymerization from the PVBC macroinitiator, the GPC chromatogram of the resulting PVBC-*b*-PS sample shows a significant shift to lower elution volume from the initial PVBC-TEMPO peak as well as an increase in molecular weight as determined by light scattering detection compared to the initial PVBC-TEMPO block. The peak shift indicates an efficient initiation from the PVBC-TEMPO macroinitiator to form the diblock copolymer.

Figure 2 depicts the ^{1}H NMR spectrum of the PVBC-*b*-PS with 0.5 h polymerization of styrene. The PVBC-*b*-PS

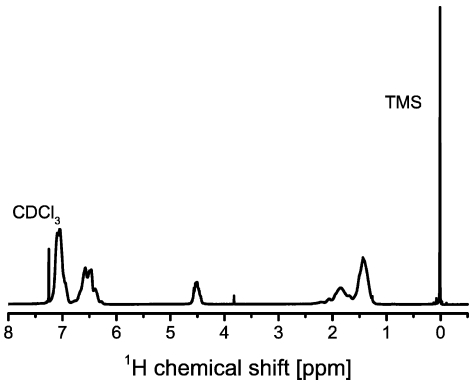

Figure 2. ^{1}H NMR spectrum of PVBC-*b*-PS by bulk copolymerization.

copolymer was reprecipitated in methanol several times to remove residual styrene monomer before ^{1}H NMR spectroscopy analysis. The spectrum exhibits both PVBC and PS characteristic peaks, and the composition can be determined by the peak ratios. The amount of PVBC in the diblock can be calculated from integration of the benzyl peaks at 4.2−4.8 ppm. The determination of the amount of PS in the diblock is complicated, as the aromatic peaks of both the PVBC and PS overlap. However, by subtracting the molar amount of PVBC aromatic peaks determined from the benzyl peaks, the amount of PS can be determined. The relative composition of PVBC and PS can be calculated by comparing the molar amount of PVBC and PS. The mass ratio of PVBC:PS is calculated to be 32:68, in good agreement with the mass ratio determined by GPC.

PPO and PS are well-known to be miscible at all compositions, and the miscibilities of a large number of polystyrene derivatives and polystyrene copolymers with PPO have been studied to find compatibility over a composition range.[58−62] The miscibility of PVBC with PPO and PVBC-*b*-PS with PPO, however, has not been reported. Because our objective is to form blends of copolymer with PPO, it was important to study the miscibility of these three different components in a blend.

The first thing to investigate was the miscibility of the PVBC-*b*-PS copolymer. The glass transition temperatures of PVBC and PS homopolymers with similar molecular weights as in the copolymer were measured by DSC to be 121 and 97 °C, respectively. The glass transition temperatures of PVBC and PS homopolymers are displayed in Figure 3 and clearly depict the

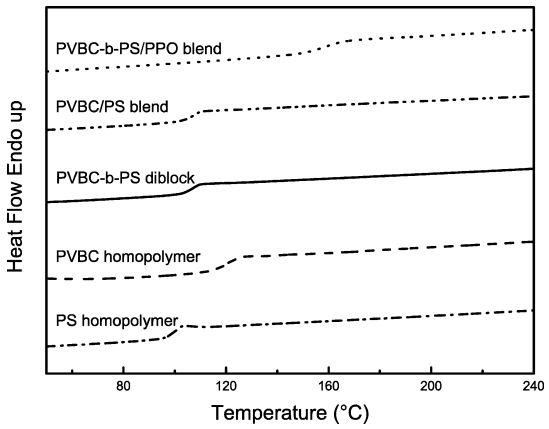

Figure 3. DSC traces of PVBC homopolymer, PS homopolymer, PVBC-*b*-PS diblock, PVBC/PS (30/70) blend, and PVBC-*b*-PS/PPO (50/50) blend membranes.

two distinct transitions. The DSC curve for PVBC-*b*-PS copolymer displays only one glass transition at 107 °C, indicating the compatibility of PVBC and PS. A PVBC/PS blend of the two homopolymers was prepared at the same composition as the PVBC-*b*-PS copolymer in order to further investigate the miscibility of PVBC and PS at this particular composition. The homopolymer blend also shows only a single glass transition in the DSC trace at a similar temperature value, suggesting that PVBC and PS are miscible at this composition.

The miscibility of PPO and the PVBC-*b*-PS was also evaluated. The glass transition temperature of PPO was measured to be 223 °C. The PPO homopolymer was then blended with the PVBC-*b*-PS copolymer in a range of compositions for the miscibility study. DSC was used to examine each PVBC-*b*-PS/PPO blend, and only one glass transition temperature is observed in each of the blends. The glass transition temperature increases with the increase in PPO composition of the blend films, as expected. Figure 3 depicts one example of the PVBC−PS/PPO blend films with 50 wt % of PPO, and the glass transition temperature of this particular blend membrane occurs at 153 °C.

The glass transition temperatures of PVBC-*b*-PS/PPO blends are plotted as a function of PPO loading contents (wt %), and the trend can be observed in Figure 4. The T_g of the miscible blend can be predicted by the Fox equation

dx.doi.org/10.1021/ma500993s | *Macromolecules* XXXX, XXX, XXX−XXX

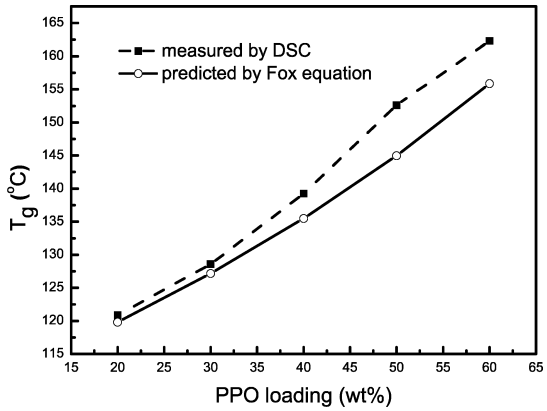

Figure 4. Measured T_g values (dashed) of PPO/PS-*b*-PVBC and theoretical values (solid) versus PPO loading (using T_g of 107 °C for the block copolymer).

$$\frac{1}{T_g} = \sum_{i=1}^{n} \frac{w_i}{T_{g,i}}$$

where w_i is the mass composition of one blend component and $T_{g,i}$ is the glass transition temperature of that component in the blend. The theoretical T_g values of the PPO blend predicted by the Fox equation show a close match with the measured values, also indicating the PPO is compatible with PVBC-*b*-PS in the concentration range investigated.

PPO was blended with PVBC-*b*-PS copolymer to prepare blend films (PVBC-*b*-PS/PPO) by solvent casting. The PVBC-*b*-PS copolymer and PPO homopolymer (M_n = 20 000 g/mol) were dried in a vacuum oven overnight and then weighed into 20 mL vials with the range of blend compositions in Table 1.

Table 1. PVBC-*b*-PS/PPO Blends Composition, Theoretical IEC, and Titrated IEC

AEM	PVBC-*b*-PS (wt %)	PPO (wt %)	theor IEC[a] (mmol/g)	titrated IEC[b] (mmol/g)
A	40	60	0.82	0.75
B	50	50	1.01	0.87
C	60	40	1.20	1.02
D	70	30	1.39	1.17
E	80	20	1.57	1.34

[a]Estimated by ^{1}H NMR spectrum and blend ratio. [b]Determined by back-titration of blended membranes after OH^- counterion exchange.

Polymer blends were prepared with concentration of 5 g/100 mL in chloroform, and sonication was applied to dissolve the polymers. The solutions were drop-cast onto glass slides, the solvent was evaporated, and the transparent films were separated from the glass slides by soaking in water.

The drop-cast PVBC-*b*-PS/PPO films were converted to quaternary ammonium-functionalized membranes. The films were immersed in methanol and the benzyl chloride groups converted to quaternary ammonium groups through reaction with trimethylamine. A large excess of trimethylamine gas was introduced to the reaction vessel in order to reach a high reaction conversion. The blend membranes were allowed to react for 48 h and became less transparent over time. The resulting membranes (P[VBTMA][Cl]-*b*-PS/PPO) were washed with water and vacuum-dried at 40 °C overnight.

The membranes were characterized by FT-IR spectroscopy, and the spectra confirmed the formation of quaternary ammonium cations in the membrane. Figure 5b depicts the

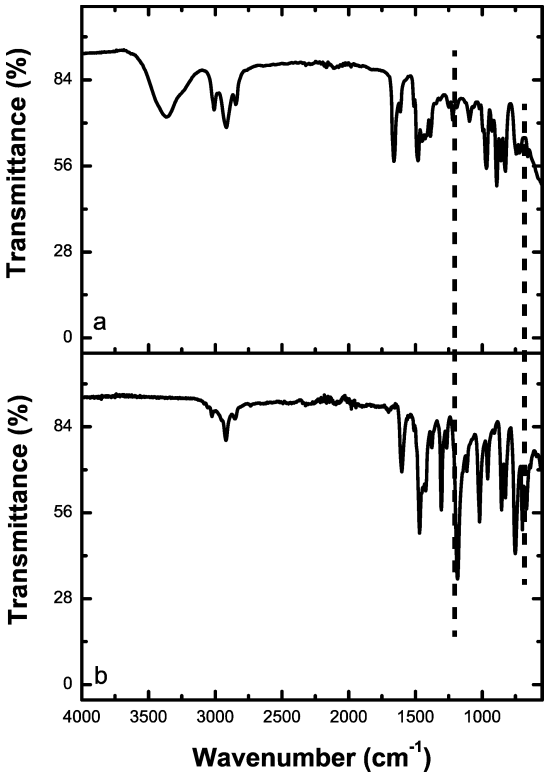

Figure 5. FT-IR spectra of (a) PVBC-*b*-PS/PPO after quaternization and (b) P[VBTMA][Cl]-*b*-PS/PPO before quaternization.

IR spectrum of PVBC-*b*-PS/PPO, showing clear chloromethyl ($-CH_2-Cl$) functional group absorption peaks at 571 and 1224 cm^{-1}. After the quaternization reaction, the absorption peaks at 571 and 1224 cm^{-1} have almost completely disappeared, indicating reaction of the chloromethyl ($-CH_2-Cl$) functional group. The strong peak at 3365 cm^{-1} in Figure 5a represents the water peak associated with the formation of the hygroscopic quaternary ammonium groups.

The ion exchange capacities (IECs) of the blend membranes were measured by hydroxide back-titration[37] and are presented in Table 1. The hydroxide ion exchange was done in 1 M degassed KOH solution for 48 h, and the excess hydroxide was removed by washing with DI water. The completion of quaternization reaction can be estimated by comparing the actual IEC with the theoretical IEC, which can be easily calculated by assuming the complete conversion of benzyl chloride groups into quaternary ammonium functional groups. The conversion to quaternary ammonium reached 84–91% for the different membranes.

The obtained PPO blend AEMs were noticeably more flexible compared to a quaternized film of P[VBTMA][Cl]-*b*-PS copolymer with no PPO added (obtained by soaking the PVBC-*b*-PS copolymer in aqueous trimethylamine solution for 48 h). In order to quantitatively examine the effects of PPO content and water absorption on mechanical performance,

dx.doi.org/10.1021/ma500993s | *Macromolecules* XXXX, XXX, XXX–XXX

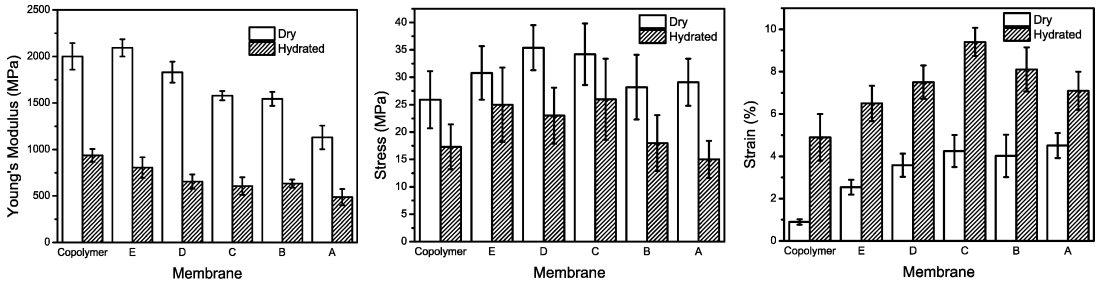

Figure 6. Young's modulus, stress at break, and strain at break of PPO blend membranes at room temperature under dry and hydrated conditions (PPO content increases from left to right for each figure).

tensile properties (Young's modulus, stress and strain at break) of the various compositions of PPO blend AEMs were measured at room temperature under both dry and hydrated conditions (Figure 6). Replicate measurements were performed for each sample to obtain average values. For membranes tested at dry condition, the Young's modulus decreased from roughly 2 to 1 GPa going from 0 to 60 wt % PPO in the blend, and the elongation at break (0.9−4.5%) generally increased when the PPO content increased, consistent with known properties of PS/PPO blends.[21,63,64] The stress at break for the dry films did not vary greatly over the series (25.9−35.4 MPa). The hydrated blend membranes show a noticeable change in tensile properties from those measured under a dry condition. The hydrated membranes display significantly lower Young's modulus and a lower stress at break (ranging from 15 to 26 MPa) as well as higher elongation at break (ranging from 4.9% to 9.4%) than their dry analogues. Water in the quaternized membrane can act as a plasticizer to decrease the modulus and increase the membrane elongation.[65] The Young's moduli for the hydrated membranes are found to decrease from 945 to 488 MPa as the PPO loading increases. However, a less clear trend is observed for stress and elongation at break data from the hydrated membranes, and membrane C (40 wt % PPO loading) shows the highest elongation at break of 9.4%. It is proposed that the stress and strain at break for the hydrated blends are dependent on both the PPO content and any plasticization from the water content. The membranes with higher PPO content also have lower water uptake and are therefore less influenced by water plasticization, while the membranes with lower PPO content have higher water uptake and more water plasticization. The two effects are seen in the strain at break data, where the balance of PPO content and water plasticization results in membrane C having the largest strain at break.

After demonstrating that blending PPO with the copolymer can lead to beneficial mechanical properties, the phase morphology and its effect on conductivity and water uptake of the quaternized membranes were investigated. The original three-component miscible blend (PVBC-*b*-PS/PPO) is expected to become incompatible, as the benzyl chloride groups of the PVBC block are converted to benzyltrimethylammonium cationic groups to form a P[VBTMA][Cl] block. The new functionalized material should now comprise a miscible blend between the PPO and the PS block with the now hydrophilic cationic P[VBTMA][Cl] immiscible with the blend. However, the phase separation between the hydrophilic and hydrophobic components is restricted because the high glass transition temperature of the PS/PPO blend does not allow reorganization of the structure at low temperatures. It is expected that an organized, phase-separated morphology could have a positive effect on anion exchange membrane conductivity;[13,43] therefore, experiments were designed to anneal the PPO blend membranes under different conditions and then to examine their conductivity and water uptake and attempt to relate the properties to a resulting phase morphology.

In order to maximize the phase separation of hydrophilic and hydrophobic components in the blend membranes, thermal and solvent vapor annealing methods were selected under both dry and humidified conditions. PS/PPO is a well-studied blend system, and the blend glass transition temperature can be predicted by the Fox equation (Table 2). The thermal

Table 2. T_g of PVBC-*b*-PS/PPO and PPO/PS after Quaternization Reaction and Annealing Conditions[a] of P[VBTMA][Cl]-b-PS/PPO Membrane

AEM	T_g[b] of PS/PPO (°C)	boil in water[c] (°C)	anneal with water[d] (°C)	anneal without water[d] (°C)	anneal over THF/water[e] (°C)
A	157	94	140	140	70
B	145	94	140	140	70
C	135	94	140	140	70
D	125	94	135	135	70
E	116	94	125	125	70

[a]All annealing methods were conducted for 12 h. [b]T_g of PS/PPO after quaternization and calculated by Fox equation for the PPO/PS system. [c]Calculated based on the elevation. [d]Determined by both predicted T_g for PPO/PS and degradation temperature from TGA. [e]Temperature was directly obtained from oil bath.

annealing temperatures for P[VBTMA][Cl]-*b*-PS/PPO membranes are required to be lower than the degradation temperature, while approaching the glass transition temperature of PS/PPO if possible. Annealing in the presence of water was expected to increase the volume of the hydrophilic component. Since the thermal stability of P[VBTMA][Cl]-*b*-PS/PPO is important to determine the annealing temperature, the thermal stability of P[VBTMA][Cl]-*b*-PS/PPO was first examined by thermogravimetric analysis (TGA). The derivative curve of the thermogravimetric trace (DTG) (Figure 7) shows three main degradation regions. The beginning of the first decomposition region starts at 143 °C, presumably corresponding to the degradation of the benzyltrimethylammonium chloride group, and indicates the upper limit for thermal annealing temperatures of the P[VBTMA][Cl]-*b*-PS/PPO membranes. Because the P[VBTMA][Cl]-*b*-PS/PPO membrane starts to degrade at 143 °C, thermal annealing temperatures were chosen to be

dx.doi.org/10.1021/ma500993s | *Macromolecules* XXXX, XXX, XXX−XXX

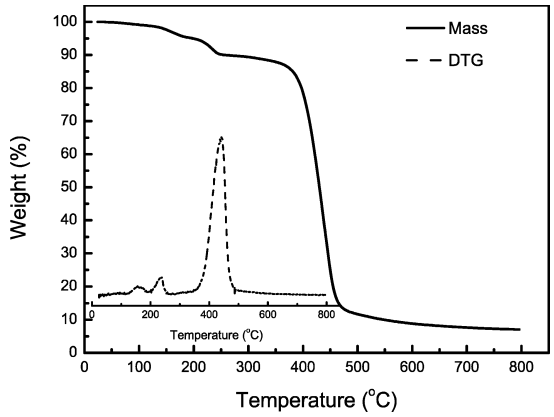

Figure 7. TGA and DTG (inset) curves of P[VBTMA][Cl]-*b*-PS/PPO.

lower than the degradation temperature. Solvent and water vapor annealing conditions were also examined as a way to avoid the higher temperatures where thermal degradation occurs.

Four separate annealing methods were investigated for the membrane films in the chloride form (Table 2): (1) annealing in boiling water; (2) at 125−140 °C without water; (3) under pressure in the presence of water at 125−140 °C; (4) solvent vapor annealing over a 50/50 mixture of THF/water. The simplest method was to boil the blend membranes in water, but the temperature of boiling water (94 °C at altitude) does not approach the glass transition temperature of the hydrophobic component (PS/PPO). Membranes were annealed at higher temperatures (125−140 °C) under pressure in the presence of water. For the samples with lower PPO composition (C, D, and E) the annealing temperature was above the T_g. For comparison, membranes were annealed at high temperatures (125−140 °C) without water. Solvent vapor annealing was investigated over a THF/water mixture to plasticize the PS/PPO component while also providing a hydrated environment for the hydrophilic component.

After thermal annealing, the IECs were remeasured for each membrane to investigate the stability of the cationic group. The titrated IECs of membranes after annealing were determined by hydroxide back-titration and are compared with the values before annealing. No measurable change is observed in the IECs after any of the annealing techniques, implying a low occurrence of either thermal degradation or leaching of hydrophilic component from the membrane.

All blend membranes before and after annealing were investigated by SAXS at 60 °C by sweeping the relative humidity (RH) from 25% to 95% RH. All as-cast blend membranes prior to annealing exhibited no features in the SAXS profiles as expected from casting the films as compatible blends followed by subsequent quaternization. Surprisingly, most of the membranes after different thermal treatments also exhibited no noticeable features in the SAXS. Only the THF/water annealed sample with the highest ion exchange capacity (sample E) displayed a significant scattering peak after annealing. The other THF/water annealed membranes (A−D) showed mostly featureless profiles, with only sample D

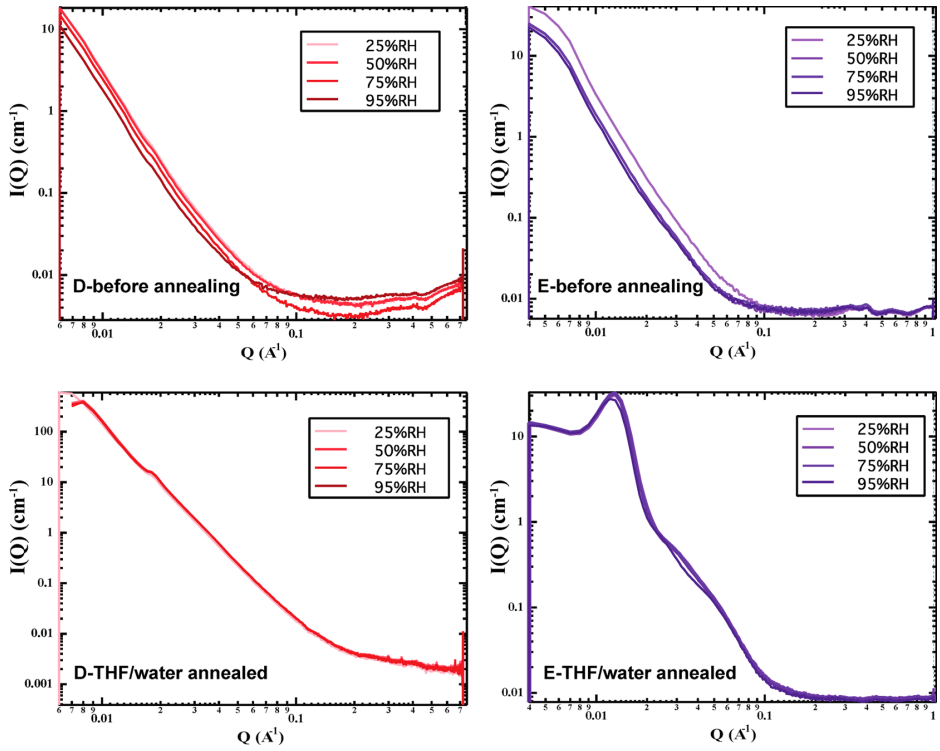

Figure 8. SAXS profiles (60 °C) of membranes D and E before and after THF/water annealing.

dx.doi.org/10.1021/ma500993s | *Macromolecules* XXXX, XXX, XXX−XXX

showing some change after annealing and a small scattering peak. The higher T_g of the membranes with higher PPO content presumably restricts the reorganization and phase separation of the membranes, and only membranes D and E are able to reorganize to a larger extent under the conditions examined. The SAXS profiles of membranes D and E are presented in Figure 8 as representatives to illustrate the effect of THF/water annealing. Figure 8 indicates an amorphous morphology in membranes D and E before annealing, corresponding to the initially miscible PVBC-*b*-PS/PPO blend. In contrast, the THF/water annealed membrane E displayed an ordered phase separation with a distinct peak at q = 0.013 A^{-1} and broad second- and third-order peaks at approximately q = 0.024 and 0.050 A^{-1}. The cluster size is determined to have a R_g of 19.1 nm and a distance between clusters of 43.7 nm. The packing factor is 7.2. Additionally, all SAXS profiles showed little response to changes in humidity, revealing that the PPO blend AEMs possess desired dimensional stability under changing humidity conditions.

HAADF STEM was performed on membrane E (nonannealed, water annealed, and THF/water annealed) and on membrane D after THF/water vapor annealing. In general, no evidence of microphase separation was observed for low- or high-temperature water annealing. Only annealing with THF/water vapor produced structures identifiable by TEM, as shown in Figure 9. HAADF STEM of the membrane E sample after

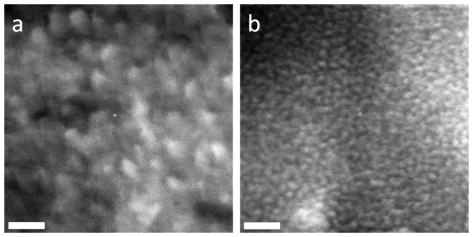

Figure 9. STEM images (scale bar 100 nm) of THF/water annealed samples (a) membrane D and (b) membrane E.

THF/water annealing revealed a fairly well-defined, microphase-separated morphology of roughly spherical domains distributed with liquid-like disorder (Figure 9b). These domains have a higher electron density than the surrounding material, indicating that they are composed of the hydrophilic, bromine-containing PVBTMA material, with a domain size of approximately 25 nm. This uniformity of structure gives rise to the Bragg diffraction peak observed by SAXS. THF/water vapor annealing also resulted in observable microphase separation for the membrane D sample, as shown in Figure 9a. Unlike the blend membrane E, the microphase-separated domains in the THF/water annealed membrane D were larger and show substantial variation in size, shape, and spatial arrangement, consistent with the general absence of characteristic features in the SAXS data.

The water uptake of all blend membranes before and after the different annealing conditions were measured at room temperature in the chloride form and compared (Figure 10a). The total number of ionic groups (as measured by IEC) varies with the amount of PPO in the blend. The water uptake is found to increase with an increase in IEC, as expected, and the membranes before annealing show the water uptake increases from 9% to 28% as the amount of PPO in the blend decreases.

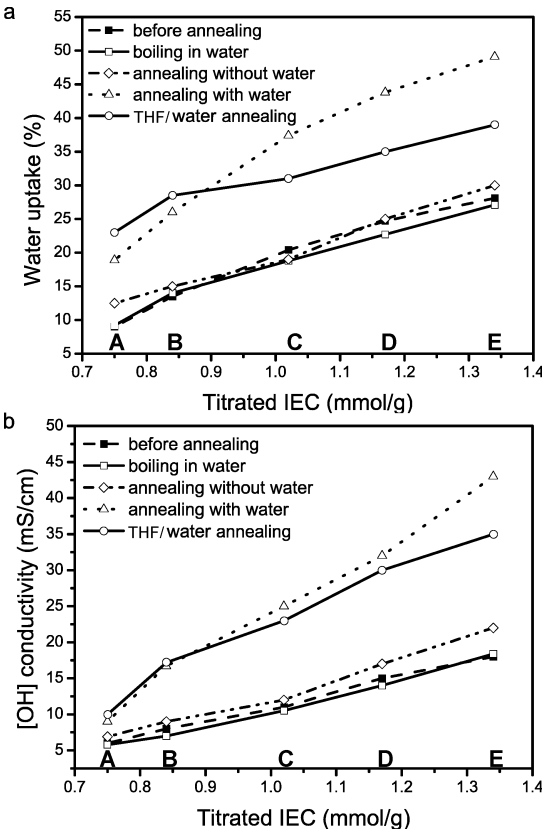

Figure 10. Water uptake (a) and hydroxide conductivity (b) comparison of membranes before and after annealing methods versus IEC.

A comparison between annealing methods reveals that almost no change occurs for samples boiled in water or for samples annealed at high temperature in the absence of water. Only the samples that were annealed at high temperature in the presence of water or over THF/water solutions showed any dramatic change in the water uptake. The change is related to these two annealing techniques allowing the rearrangement of the PPO/PS blend while also hydrating the hydrophilic component to increase its volume fraction.

Conductivities of all membranes were measured in both the hydroxide and chloride forms at 60 °C in water by electrochemical impedance spectroscopy. Similar to water uptake, the ionic conductivity is found to increase with increasing IEC for both hydroxide and chloride form (Figure 10b), and the detailed conductivity data are listed in Table 3. The hydroxide conductivities are 2−4 times higher than chloride conductivities for all membranes as observed in other work.[45,66] Also similar to the water uptake results, annealing at high temperature in the presence of water or over THF/water solutions exhibited a significant effect on the membrane ionic conductivity, while membranes boiled in water or annealed at high temperature in the absence of water show little change in conductivity. Hydroxide conductivity of membrane E (IEC = 1.34 mmol/g) increases from 16 to 43 mS/cm on going from nonannealed membrane to after high-temperature water annealing, which is consistent with the trend

dx.doi.org/10.1021/ma500993s | *Macromolecules* XXXX, XXX, XXX−XXX

Table 3. Conductivity[a] (Hydroxide and Chloride[b]) Comparison between Membranes before and after Annealing

AEM	IEC (mmol/g)	σ_0 (mS/cm)	σ_1 (mS/cm)	σ_2 (mS/cm)	σ_3 (mS/cm)	σ_4 (mS/cm)
A	0.75	6.0 (1.9)	5.8 (1.7)	6.9 (2.0)	9.0 (3.0)	10 (3.6)
B	0.87	8.0 (2.1)	7.0 (2.5)	9.0 (3.5)	17 (4.9)	17 (4.7)
C	1.02	11 (3.9)	11 (3.4)	12 (4.3)	25 (6.3)	23 (7.0)
D	1.17	15 (5.5)	14 (6.2)	17 (7.2)	32 (13)	30 (11)
E	1.34	18 (8.0)	18 (8.6)	22 (10)	43 (18)	35 (13)

[a]The subscripts of IEC stand for the annealing methods: 0 represents the membranes before annealing; 1 represents the membranes after boiling in water; 2 represents the membranes after annealing at high temperature without water; 3 represents the membranes after annealing at high temperature with water; 4 represents the membranes after annealing with THF/water. [b]Chloride conductivity is in parentheses.

observed in water uptake. The effect of ionic conductivity with increased water uptake indicates that the conductivity is highly dependent on the water uptake.

In order to get a better understanding of conductivity variation of the membranes with different annealing conditions, hydroxide conductivity of the membranes before and after annealing (THF/water and water at high temperature) as a function of water uptake is plotted in Figure 11. Regardless of

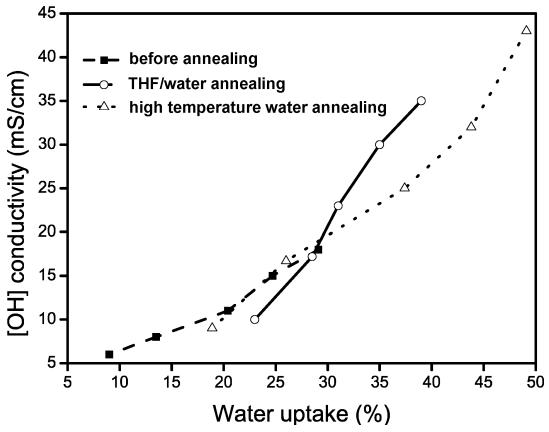

Figure 11. Hydroxide conductivities of membranes before and after annealing as a function of water uptake. The lowest conductivity points for each series are membrane A, and the highest for each series are membrane E.

annealing method, the membranes show both increased water uptake and increased hydroxide conductivity with an increase in IEC, such that for a given annealing method, the lowest data point in Figure 11 is membrane A and the highest data point is membrane E. A close comparison reveals that membranes with similar water uptake display comparable conductivity. For instance, membrane E before annealing (water uptake = 28.1%) displays a similar water uptake as membrane B after THF/water annealing (water uptake = 28.5%), and they have similar conductivity values; however, the IEC differences between membranes E (IEC = 1.34 mmol/g) and B (IEC = 0.87 mmol/g) are quite significant. In addition, high temperature water annealing produced the membrane with the greatest water uptake and the highest conductivity, but the membranes annealed by THF/water exhibited a different conductivity versus water uptake relationship, whereby a relatively higher conductivity is observed for a given water uptake. This implies that the THF/water annealed membrane can use water more efficiently, which could be a result of the development of more conducting pathways along with the increase in water volume. Overall, water uptake appears to be more important for high conductivity than does a highly organized phase-separated morphology.

Having determined that membranes D and E annealed by either high temperature water annealing or by annealing over THF/water solutions show the best conductivity properties, the tensile mechanical properties of the annealed samples were examined (Figure 12). However, no measurable differences were determined from that of the unannealed samples.

CONCLUSION

We have demonstrated the preparation of AEMs by blending PPO with PVBC-*b*-PS to form miscible blends followed by subsequent trimethylamine quaternization. The addition of PPO improves the mechanical properties over that of the styrenic block copolymer. Annealing of the blend membranes is necessary to obtain good conductivity values because of the way the films are cast as miscible blends and then converted into quaternary ammonium-functionalized materials. Only the annealing procedures that provide both a hydrated environment for the cationic component and conditions where the high T_g matrix can reorganize are effective for increasing both the water uptake and the conductivity. While no strong

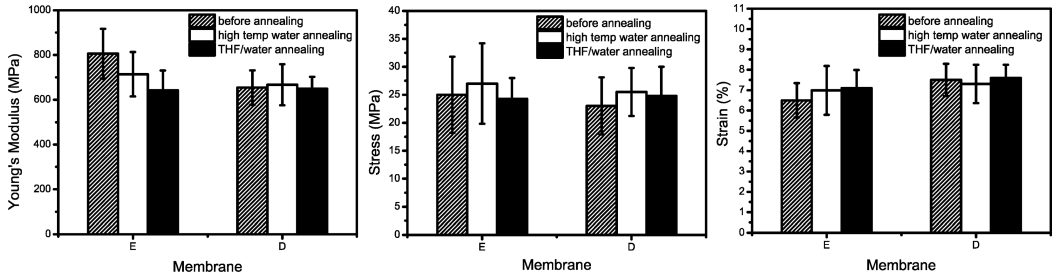

Figure 12. Tensile properties of membranes D and E before and after annealing.

dx.doi.org/10.1021/ma500993s | Macromolecules XXXX, XXX, XXX−XXX

correlation of conductivity with morphology is determined for these membranes, the blend membrane with a more organized phase-separated morphology is observed to require less water to display a high conductivity.

AUTHOR INFORMATION

Corresponding Author

*E-mail: dknauss@mines.edu (D.M.K.).

Notes

The authors declare no competing financial interest.

ACKNOWLEDGMENTS

This work was funded by the Army Research Office through a MURI (grant # W911NF-10-1-0520). NMR spectroscopy was made possible through a grant from the NSF MRI program (grant # CHW-0923537). A.C.J. was supported by the Postgraduate Research Participation Program at the US Army Research Laboratory, administered by the Oak Ridge Institute of Science and Education through an interagency agreement between the US Department of Energy and Army Research Laboratory (Contract ORISE 1120-1120-99). The authors also thank Blake Whitley and Prof. Kip Findley for their assistance with membrane tensile tests. The use of the Advanced Photon Source, an Office of Science User Facility operated for the US Department of Energy (DOE) Office of Science by Argonne National Laboratory, was supported by the US DOE under contract DE-AC02-06CH11357.

REFERENCES

(1) McLean, G. F.; Niet, T.; Prince-Richard, S.; Djilali, N. *Int. J. Hydrogen Energy* **2002**, *27*, 507.
(2) Varcoe, J. R.; Slade, R. C. T. *Fuel Cells* **2005**, *5*, 187.
(3) Sanabria-Chinchilla, J.; Asazawa, K.; Sakamoto, T.; Yamada, K.; Tanaka, H.; Strasser, P. *J. Am. Chem. Soc.* **2011**, *133*, 5425.
(4) Gülzow, E. *Fuel Cells* **2004**, *4*, 251.
(5) Gülzow, E. *J. Power Sources* **1996**, *61*, 99.
(6) Merle, G.; Wessling, M.; Nijmeijer, K. *J. Membr. Sci.* **2011**, *377*, 1.
(7) Couture, G.; Alaaeddine, A.; Boschet, F.; Ameduri, B. *Prog. Polym. Sci.* **2011**, *36*, 1521.
(8) Jaeger, W.; Bohrisch, J.; Laschewsky, A. *Prog. Polym. Sci.* **2010**, *35*, 511.
(9) Einsla, B. R.; Chempath, S.; Pratt, L.; Boncella, J.; Rau, J.; Macomber, C.; Pivovar, B. *ECS Trans.* **2007**, *11*, 1173.
(10) Hibbs, M. R.; Hickner, M. A.; Alam, T. M.; McIntyre, S. K.; Fujimoto, C. H.; Cornelius, C. J. *Chem. Mater.* **2008**, *20*, 2566.
(11) Zhou, J.; Unlu, M.; Vega, J. A.; Kohl, P. A. *J. Power Sources* **2009**, *190*, 285.
(12) Yan, J.; Hickner, M. A. *Macromolecules* **2010**, *43*, 2349.
(13) Tanaka, M.; Fukasawa, K.; Nishino, E.; Yamaguchi, S.; Yamada, K.; Tanaka, H.; Bae, B.; Miyatake, K.; Watanabe, M. *J. Am. Chem. Soc.* **2011**, *133*, 10646.
(14) Hibbs, M. R.; Fujimoto, C. H.; Cornelius, C. J. *Macromolecules* **2009**, *42*, 8316.
(15) Kostalik, H. A.; Clark, T. J.; Robertson, N. J.; Mutolo, P. F.; Longo, J. M.; Abruña, H. C. D.; Coates, G. W. *Macromolecules* **2010**, *43*, 7147.
(16) Noonan, K. J. T.; Hugar, K. M.; Kostalik, H. A.; Lobkovsky, E. B.; Abruña, H. D.; Coates, G. W. *J. Am. Chem. Soc.* **2012**, *134*, 18161.
(17) Slade, R. C. T.; Varcoe, J. R. *Solid State Ionics* **2005**, *176*, 585.
(18) Varcoe, J. R.; Slade, R. C. T.; Lam How Yee, E.; Poynton, S. D.; Driscoll, D. J.; Apperley, D. C. *Chem. Mater.* **2007**, *19*, 2686.
(19) Zeng, Q. H.; Liu, Q. L.; Broadwell, I.; Zhu, A. M.; Xiong, Y.; Tu, X. P. *J. Membr. Sci.* **2010**, *349*, 237.
(20) Tsai, T.-H.; Maes, A. M.; Vandiver, M. A.; Versek, C.; Seifert, S.; Tuominen, M.; Liberatore, M. W.; Herring, A. M.; Coughlin, E. B. *J. Polym. Sci., Part B: Polym. Phys.* **2013**, *51*, 1751.
(21) Hay, A. S. *J. Polym. Sci., Part A: Polym. Chem.* **1998**, *36*, 505.
(22) Puskas, J. E.; Kwon, Y.; Altstädt, V.; Kontopoulou, M. *Polymer* **2007**, *48*, 590.
(23) Li, N.; Leng, Y.; Hickner, M. A.; Wang, C.-Y. *J. Am. Chem. Soc.* **2013**, *135*, 10124.
(24) Rebeck, N. T.; Li, Y.; Knauss, D. M. *J. Polym. Sci., Part B: Polym. Phys.* **2013**, *51*, 1770.
(25) Tongwen, X.; Weihua, Y. *J. Membr. Sci.* **2001**, *190*, 159.
(26) Wu, L.; Xu, T.; Wu, D.; Zheng, X. *J. Membr. Sci.* **2008**, *310*, 577.
(27) Wu, L.; Xu, T.; Yang, W. *J. Membr. Sci.* **2006**, *286*, 185.
(28) Bair, H. E. *Polym. Eng. Sci.* **1970**, *10*, 247.
(29) Oudhuis, A. A. C. M.; Ten Brinke, G. *Macromolecules* **1992**, *25*, 698.
(30) Shultz, A. R.; Gendron, B. M. *J. Appl. Polym. Sci.* **1972**, *16*, 461.
(31) Lefebvre, D.; Jasse, B.; Monnerie, L. *Polymer* **1981**, *22*, 1616.
(32) Tucker, P. S.; Barlow, J. W.; Paul, D. R. *Macromolecules* **1988**, *21*, 1678.
(33) Yang, J.; An, L.; Xu, T. *Polymer* **2001**, *42*, 7887.
(34) Mazard, C.; Benyahia, L.; Tassin, J.-F. *Polym. Int.* **2003**, *52*, 514.
(35) Li, G. H.; Lee, C. H.; Lee, Y. M.; Cho, C. G. *Solid State Ionics* **2006**, *177*, 1083.
(36) Cho, C. G.; Kim, S. H.; Park, Y. C.; Kim, H.; Park, J.-W. *J. Membr. Sci.* **2008**, *308*, 96.
(37) Danks, T. N.; Slade, R. C. T.; Varcoe, J. R. *J. Mater. Chem.* **2003**, *13*, 712.
(38) Fujimoto, C. H.; Hickner, M. A.; Cornelius, C. J.; Loy, D. A. *Macromolecules* **2005**, *38*, 5010.
(39) Liu, Y.; Horan, J. L.; Schlichting, G. J.; Caire, B. R.; Liberatore, M. W.; Hamrock, S. J.; Haugen, G. M.; Yandrasits, M. A.; Seifert, S.; Herring, A. M. *Macromolecules* **2012**, *45*, 7495.
(40) Schlichting, G. J.; Horan, J. L.; Jessop, J. D.; Nelson, S. E.; Seifert, S.; Yang, Y.; Herring, A. M. *Macromolecules* **2012**, *45*, 3874.
(41) Park, M. J.; Nedoma, A. J.; Geissler, P. L.; Balsara, N. P.; Jackson, A.; Cookson, D. *Macromolecules* **2008**, *41*, 2271.
(42) Park, M. J.; Downing, K. H.; Jackson, A.; Gomez, E. D.; Minor, A. M.; Cookson, D.; Weber, A. Z.; Balsara, N. P. *Nano Lett.* **2007**, *7*, 3547.
(43) Elabd, Y. A.; Hickner, M. A. *Macromolecules* **2010**, *44*, 1.
(44) Weber, R. L.; Ye, Y.; Schmitt, A. L.; Banik, S. M.; Elabd, Y. A.; Mahanthappa, M. K. *Macromolecules* **2011**, *44*, 5727.
(45) Sudre, G.; Inceoglu, S.; Cotanda, P.; Balsara, N. P. *Macromolecules* **2013**, *46*, 1519.
(46) Hubner, G.; Roduner, E. *J. Mater. Chem.* **1999**, *9*, 409.
(47) Horák, Z.; Fortelný, I.; Kolařík, J.; Hlavatá, D.; Sikora, A. In *Encyclopedia of Polymer Science and Technology*; John Wiley & Sons, Inc.: New York, 2002.
(48) Stoelting, J.; Karasz, F. E.; Macknight, W. J. *Polym. Eng. Sci.* **1970**, *10*, 133.
(49) Shultz, A. R.; Beach, B. M. *J. Appl. Polym. Sci.* **1977**, *21*, 2305.
(50) Picchioni, F.; Casentini, E.; Passaglia, E.; Ruggeri, G. *J. Appl. Polym. Sci.* **2003**, *88*, 2698.
(51) Kuo, S.-W.; Huang, C.-F.; Tung, P.-H.; Huang, W.-J.; Huang, J.-M.; Chang, F.-C. *Polymer* **2005**, *46*, 9348.
(52) Wu, D.; Wang, X.; Jin, R. *J. Appl. Polym. Sci.* **2006**, *99*, 3336.
(53) Ting, W.-H.; Dai, S. A.; Shih, Y.-F.; Yang, I. K.; Su, W.-C.; Jeng, R.-J. *Polymer* **2008**, *49*, 1497.
(54) Georges, M. K.; Veregin, R. P. N.; Kazmaier, P. M.; Hamer, G. K. *Macromolecules* **1993**, *26*, 2987.
(55) Hawker, C. J. *J. Am. Chem. Soc.* **1994**, *116*, 11185.
(56) Kazmaier, P. M.; Daimon, K.; Georges, M. K.; Hamer, G. K.; Veregin, R. P. N. *Macromolecules* **1997**, *30*, 2228.
(57) Lacroix-Desmazes, P.; Delair, T.; Pichot, C.; Boutevin, B. *J. Polym. Sci., Part A: Polym. Chem.* **2000**, *38*, 3845.
(58) Shultz, A. R.; Beach, B. M. *Macromolecules* **1974**, *7*, 902.
(59) Brinke, G. T.; Karasz, F. E.; MacKnight, W. J. *Macromolecules* **1983**, *16*, 1827.
(60) Zacharius, S. L.; Ten Brinke, G.; MacKnight, W. J.; Karasz, F. E. *Macromolecules* **1983**, *16*, 381.

(61) Kambour, R. P.; Gundlach, P. E.; Wang, I.-C. W.; White, D. M.; Yeagert, G. W. *Polym. Commun.* **1988**, *29*.
(62) Vukovic, R.; Bogdanic, G. *J. Phys. Chem. Ref. Data* **1999**, *28*, 851.
(63) Fried, J. R.; MacKnight, W. J.; Karasz, F. E. *J. Appl. Phys.* **1979**, *50*, 6052.
(64) Kleiner, L. W.; Karasz, F. E.; MacKnight, W. J. *Polym. Eng. Sci.* **1979**, *19*, 519.
(65) Fujimoto, C.; Kim, D.-S.; Hibbs, M.; Wrobleski, D.; Kim, Y. S. *J. Membr. Sci.* **2012**, *423*−*424*, 438.
(66) Robertson, N. J.; Kostalik, H. A.; Clark, T. J.; Mutolo, P. F.; Abruña, H. D.; Coates, G. W. *J. Am. Chem. Soc.* **2010**, *132*, 3400.